NJC

PAPER

View Article Online
View Journal | View Issue

Cite this: *New J. Chem.*, 2016, **40**, 4160

Synthesis and structural characterization of Zn-containing DAF-1†

Ana B. Pinar,[a] Lynne B. McCusker,*[a] Christian Baerlocher,[a] Son-Jong Hwang,[b] Dan Xie,[c] Annabelle I. Benin[c] and Stacey I. Zones[c]

Received (in Nottingham, UK) 19th October 2015,
Accepted 27th November 2015

DOI: 10.1039/c5nj02897c

www.rsc.org/njc

A study exploring the use of ionic liquid reactions based on imidazolium halides in molecular sieve synthesis has produced a novel zincoaluminophosphate material with an open **DFO**-type framework structure. This framework structure had only been observed previously in the magnesioaluminophosphate system (Mg-DAF-1) where decamethonium was used as the structure directing agent. The new Zn-DAF-1 material has been characterized using chemical and thermogravimetric analysis and ^{13}C, ^{19}F, ^{27}Al and ^{31}P MAS NMR techniques. Structure analysis (*P6/mcc*, a = 22.2244(1) Å, c = 42.3293(3) Å) using synchrotron powder diffraction data not only confirmed the framework structure, but also revealed the locations of the Al, P and Zn atoms in the framework, the *N,N′*-di-isopropyl-imidazolium (DIPI) ions in the pores, some fluoride ions associated with double 4-rings, and some water molecules and anions filling the remaining space. This level of structural detail had not been possible in the Mg-DAF-1 material. Four different locations for the DIPI cation were found in the two 12-ring channels and Zn was found to substitute for only one of the six crystallographically distinct Al sites to yield the approximate crystal chemical formula $|(DIPI)_{17}(OH,F)_{11}(H_2O)_{23}|[Zn_6Al_{126}P_{132}O_{528}]$-**DFO**.

Introduction

A novel zincoaluminophosphate material was obtained during the course of a study exploring the use of ionic liquid reactions based upon imidazolium halides. The use of such reaction media for the crystallization of molecular sieves was pioneered by Morris and co-workers some ten years ago.[1] In their early work they created novel AlPO-based materials like SIZ-3.[2] In this chemistry, the inorganic reactants are added to the imidazolium halide and the components are heated for selected periods of time. The imidazolium compound serves as both a solvent and a guest molecule (Structure Directing Agent or SDA), filling the pores of the crystalline inorganic lattice as it grows.

While the imidazolium halides have desirable activity as ionic liquids, supporting reactions that require polar solvation, they also have a long history as attractive SDAs, and have been used to discover novel zeolite structures or to provide better routes to known ones. Zones first showed the utility of such *N,N′* disubstituted, and hence charged, imidazolium compounds in zeolite synthesis.[3] Later Archer, working in the Mark Davis group, used a different synthetic entry point to generate a number of larger R groups bonded to the imidazolium SDA.[4] This had the consequence that better candidate SDAs to make the zeolite SSZ-70 were generated.[5] This new zeolite displays particularly interesting features that provide novel routes to delaminated surfaces. Katz and co-workers have demonstrated that these surfaces can be repopulated with selected catalytic sites that are capable of transforming substrate molecules larger than those that can be handled by most zeolite catalysts.[6,7] Most recently, imidazolium SDAs with derivatization beyond just the nitrogen atoms in the ring, have produced further breakthroughs in zeolite synthesis chemistry,[8–10] including the discovery of the novel zeolite CIT-7.[11]

Returning to their use in ionic liquid media, Morris *et al.* recently showed that the more difficult silicate syntheses could be carried out successfully using an imidazolium SDA.[12] The same group demonstrated that Me-AlPO materials, where Al is partially replaced with a divalent metal, thereby generating a charge deficiency, could also be synthesized. The latter were of interest to us, because the divalent cation creates, in essence, the possibility of an acid site in the zeolitic product. We ran experiments using the *N,N′*-di-isopropyl-imidazolium cation (DIPI), which had produced an **MTT**-type[13] zeolite in silicate reactions[4] and a borosilicate SSZ-70 in fluoride medium.[8] When we used it together with zinc in the aluminophosphate system, we produced a zincoaluminophosphate material that proved to have a **DFO**-type framework structure (Fig. 1). This is a

[a] *Laboratory of Crystallography, ETH Zurich, Zurich, Switzerland. E-mail: ana.pinar@mat.ethz.ch*
[b] *Chemical Engineering, California Institute of Technology, Pasadena, CA, USA*
[c] *Chevron ETC, Richmond, CA, USA*

† Electronic supplementary information (ESI) available: Solid state ^{13}C, ^{27}Al and ^{19}F MAS NMR spectra, Hirshfeld surfaces showing the arrangement of DIPI cations in the channels, and a crystallographic information file (CIF) for Zn-DAF-1. See DOI: 10.1039/c5nj02897c

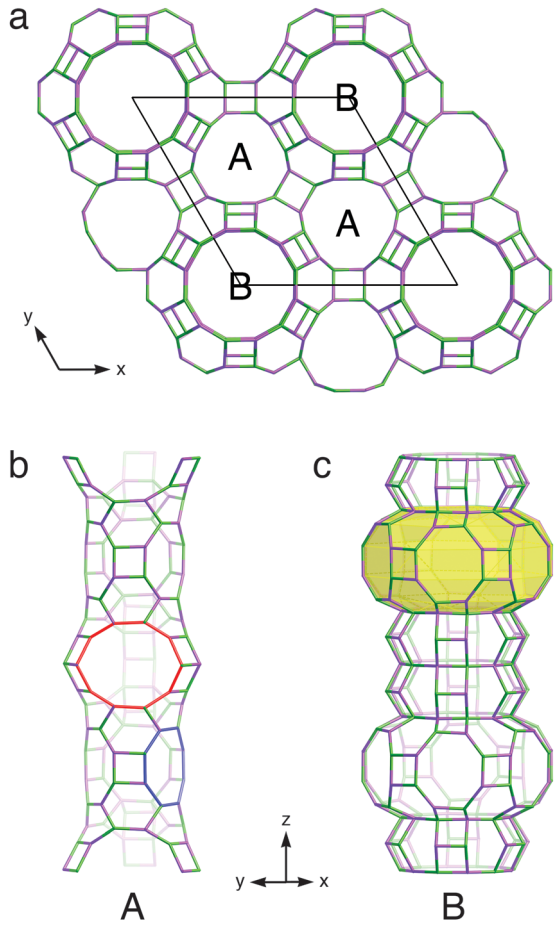

Fig. 1 Framework structure of DAF-1. (a) The arrangement of channels A and B in the projection of the framework down the *c*-axis. (b) Channel A with one 10-ring connection (red) to a neighboring channel A and one 8-ring connection (blue) to a neighboring channel B highlighted. (c) Channel B with one large cavity highlighted in yellow. Green: Al; purple: P. Framework oxygen atoms have been omitted for clarity.

novel composition for this crystalline phase, which was synthesized originally in the magnesioaluminophosphate form using conventional hydrothermal synthesis procedures and decamethonium (DM) as the SDA.[14] That Mg-DAF-1 material was found to transform to an **AFI**- or tridymite-type material upon calcination and exposure to ambient moisture. Zn-DAF-1, on the other hand, proved to be stable to calcination up to 400 °C under nitrogen.

The **DFO** framework structure (Fig. 1) has two types of 12-ring channels. One has an almost uniform cross section, whereas the second undulates, forming two types of large cavities. For the sake of simplicity, the former will be referred to as channel A and the latter as channel B. There are two channels A and one channel B per unit cell. Each channel B connects to six channels A *via* 8-ring windows. Each channel A is further connected to three channels A through 10-ring openings. In addition to the large channels, there are six double-4-ring (*d4r*) and 12 *lau* units[15] per unit cell.

To learn if there were any significant differences between Zn-DAF-1 and the original Mg-DAF-1, we were interested in determining (1) where the *N*,*N*′-di-isopropyl-imidazolium was accommodated in the **DFO** channels, (2) where the fluoride ions were located, and (3) whether it was possible to pinpoint the Zn positions in the framework. To this end, a careful structure analysis of the as-synthesized material using synchrotron powder diffraction data was undertaken.

Experimental

Synthesis

The chemical reagents used include phosphoric acid (86 wt%, Baker), hydrofluoric acid (48 wt%, Fisher), aluminum isopropoxide (98 wt%, Alfa Aesar), and zinc acetate dihydrate (Mallinckrodt). All the reagents were used without further purification. 4.5 g of *N*,*N*′-di-isopropyl-imidazolium bromide,[16] 0.42 g of zinc acetate dihydrate, and 1.15 g of aluminum isopropoxide were mixed intimately and then two liquids were added rapidly: 0.89 g of concentrated phosphoric acid, followed by 3 drops (*ca.* 0.06 g) of concentrated HF. A plastic spatula was then used to hand-mix this into a paste. The reaction mixture was heated at 160 °C for 3 days in a Teflon-lined small Parr pressure reactor tumbled at 43 rpm. The product was then filtered, washed and dried.

Chemical analysis

Chemical analysis was performed by Galbraith Laboratories, Inc. using inductively coupled plasma (ICP) methods.

MAS NMR

^{31}P MAS NMR spectra were recorded using a Bruker DSX-500 spectrometer and a 4 mm Bruker MAS NMR probe. About 60 mg of powder sample was packed into a 4 mm zirconia rotor and spun at 14 kHz at ambient conditions. ^{31}P spin–lattice relaxation time was determined to be 31 s, and so a recycle delay time of 150 s was used during signal averaging followed by a 4 μs–π/2 pulse and a strong ^{1}H decoupling pulse. The ^{31}P shift was referenced externally to concentrated H_3PO_4. Similarly, solid state ^{13}C CPMAS, ^{27}Al and ^{19}F MAS NMR were recorded, and their shifts were referenced externally to tetramethylsilane, 1 M $Al(NO_3)_2$ and $CFCl_3$, respectively. For ^{27}Al NMR, a 0.5 μs–π/18 pulse was used.

Structure analysis

Synchrotron powder diffraction data were collected on the Materials Science Beamline at the Swiss Light Source (SLS) in Villigen, Switzerland[17] (Table 1). Rietveld refinement was performed using the XRS-82 suite of programs.[18]

Results

The as-synthesized zincoaluminophosphate product Zn-DAF-1 was characterized by chemical analysis, solid state ^{13}C, ^{27}Al and ^{19}F MAS NMR spectroscopy and X-ray powder diffraction structural analysis.

Chemical analysis

Chemical CHN analysis showed an organic content of 13.9 wt% (*ca.* 17 DIPI per unit cell), and a C/N ratio of 4.6, almost

Table 1 Synchrotron powder diffraction data collection parameters for Zn-DAF-1

Synchrotron facility	SLS
Beamline	Material science
Diffraction geometry	Debye–Scherrer
Detector	MYTHEN II
Monochromator	Si 111
Wavelength	1.000 Å
Sample	Rotating 0.3 mm capillary
Nominal step size	0.004° 2θ
Detector positions	8
Time per pattern	15 s
2θ range	2.6–43.6° 2θ

identical to that of the cation (4.5), suggesting that it remains intact within the zeolite.

MAS NMR

Solid state ^{13}C, ^{27}Al and ^{19}F MAS NMR spectra are available in the ESI.† The ^{13}C CPMAS spectrum (Fig. S1, ESI†) clearly shows that the DIPI is intact. The ^{31}P MAS spectrum (Fig. 2) shows that there are at least four distinguishable P(OAl)$_4$ sites and two broad downfield resonances that were assigned as P(OAl)$_3$(OZn) sites. The components resulting from the decomposition of the spectrum are summarized in Table 2. Based on these peak intensities, the Zn content is calculated to be 2.5 mol% and the P/Al ratio 1.05. The main ^{19}F NMR signal (Fig. S2, ESI†) is observed as a broad resonance at −140 ppm with numerous spinning sidebands. This can be ascribed to terminal fluorine (Al–F units in Al(VI) sites), as previously reported for AlPO-16.[19] A relatively sharp resonance at −93 ppm, typical of F in a *d4r*,[20] accounts for approximately 10% of the total signal. The ^{27}Al MAS spectrum shows three different coordination environments (4-, 5- and 6-coordinate at *ca.* 40 ppm, 8 ppm, and −6.3 ppm with 62%, 14%, and 24% populations, respectively). In ^{19}F–^{27}Al CPMAS NMR experiments, it was found that the F resonance at −93 ppm is coupled to 4-coordinate Al, while that at −140 ppm with 6-coordinate Al.

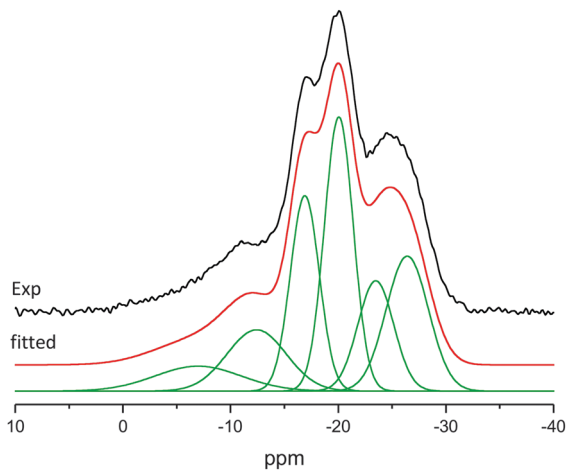

Fig. 2 ^{31}P MAS NMR spectrum of Zn-DAF-1 showing the decomposition into six components.

Table 2 Decomposition of ^{31}P MAS NMR spectrum of Zn-DAF-1

Chemical shift (ppm)	Width (Hz)	Intensity	Assignment
−6.98	1616.00	0.07	P(3AlZn)
−12.42	1111.00	0.13	P(3AlZn)
−16.89	541.58	0.19	P(4Al)
−20.05	540.02	0.27	P(4Al)
−23.48	670.08	0.14	P(4Al)
−26.41	793.68	0.20	P(4Al)

Structure analysis

The diffraction pattern of Zn-DAF-1 was indexed using the program TREOR[21] implemented in CMPR[22] to give a hexagonal unit cell (a = 22.224 Å, c = 42.329 Å), which is similar to that reported for the framework structure of Mg-DAF-1.[14] The systematic absences were compatible with the space group *P*6/*mcc*, which was also used in the more detailed Mg-DAF-1 structure analysis,[23] so structure refinement was initiated in this space group using the published atomic coordinates for the aluminophosphate framework. The framework geometry was optimized using a distance-least-squares procedure,[24] and once a good profile fit had been achieved for the higher angle region of the diffraction pattern, a difference electron density map using the whole pattern was calculated (Fig. 3). This revealed a few small clouds of electron density in the void volume of the structure. However, the high symmetry of the framework made it difficult to interpret these

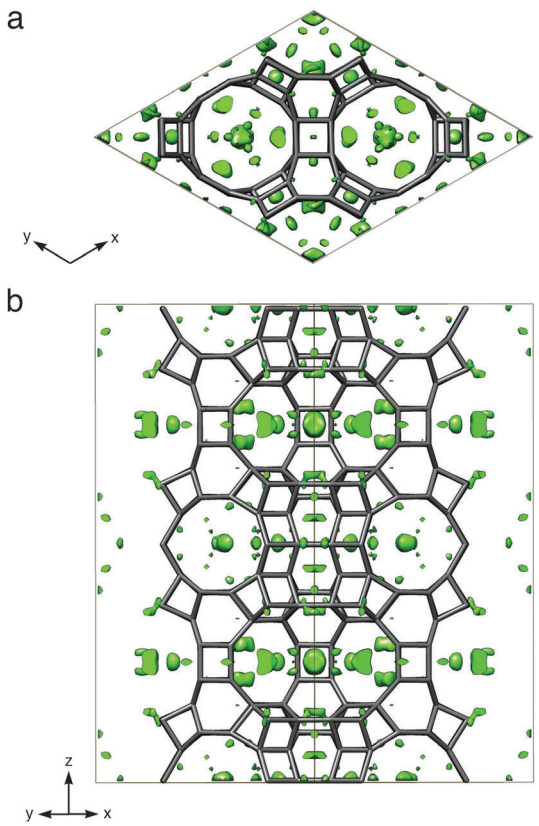

Fig. 3 Initial difference electron density map calculated with only the framework structure in the model: (a) projection down the *c*-axis and (b) projection down [110]. The framework structure is overlaid as a guide.

clouds. Therefore the selection of the initial positions and orientations of the DIPI was more a guess than a proper interpretation of the difference map. With the DIPI in the pores, however, the scale factor became more reasonable and subsequent maps revealed an electron cloud concentrated on the Al5 position. In a refinement of all the Al occupancies, Al5 was also the only one to refine to a value greater than 1, so Zn was placed at T5 and its occupancy factor was refined, restricting the total Al + Zn occupancy to 1.0. This resulted in a Zn occupancy of 0.254 (6.1 Zn per unit cell). The DIPI species were then removed from the model in the hope that the true location of the DIPIs would become clearer with this better description of the framework and a more correct scale factor. Indeed, in a series of difference electron density maps, four DIPI locations could be identified and were loaded into the model.

To describe their orientations, we define the molecular axis of the DIPI as the line passing through the two nitrogen atoms. DIPI-1 is close to the walls of the larger cavity in channel B with its molecular axis perpendicular to the *c* axis (Fig. 4). The plane of its imidazolium ring forms a *ca.* 30° angle with the *c* axis. DIPI-2 occupies the center of the same cavity, almost on the 6-fold axis, oriented with its molecular axis parallel to the *c* axis. DIPI-3 has the same orientation as DIPI-2, and lies very close to the 3-fold axis in channel A (Fig. 5). DIPI-4 is in the 10-ring aperture that connects neighboring channels A, and has an orientation similar to that of DIPI-1. Even with strong geometric restraints, attempts to refine the atomic positions of the DIPI species failed. However, by adding hard constraints to keep the imidazolium rings planar and the isopropyl moieties chemically sensible, a better positioning of the DIPI species and cleaner difference maps could be obtained.

Restraints were added to keep DIPI-1 and DIPI-4 at reasonable distances from the framework O atoms. The H atoms in the DIPI species were taken into account by increasing the population factors of the C atoms according to the number of H atoms bonded to them. The maximum occupancy factor possible for each DIPI depends on the number of equivalent positions over which the molecule is disordered, and how many of them can be occupied simultaneously. For example, the maximum occupancy of DIPI-1 is 1/4 (or 6 per unit cell) because it is disordered over 24 positions, and only six of these can be occupied at the same time. The occupancies refined to 5.0 DIPI-1, 2 DIPI-2 (maximum occupancy 2), 6.7 DIPI-3 (maximum occupancy 8) and 3.5 DIPI-4 (maximum occupancy 6) per unit cell. This adds up to 17.2 DIPI occupying the 22 positions available per unit cell.

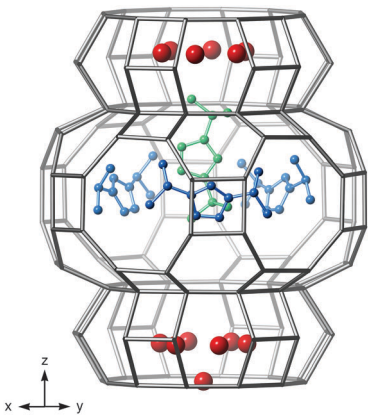

Fig. 4 Channel B showing a possible arrangement of DIPI-1 (blue) and DIPI-2 (green) in the large cavity and the water molecules in the smaller cavity (red balls). Note that only half of the unit cell (along *c*) is shown. Framework oxygen atoms have been omitted for clarity.

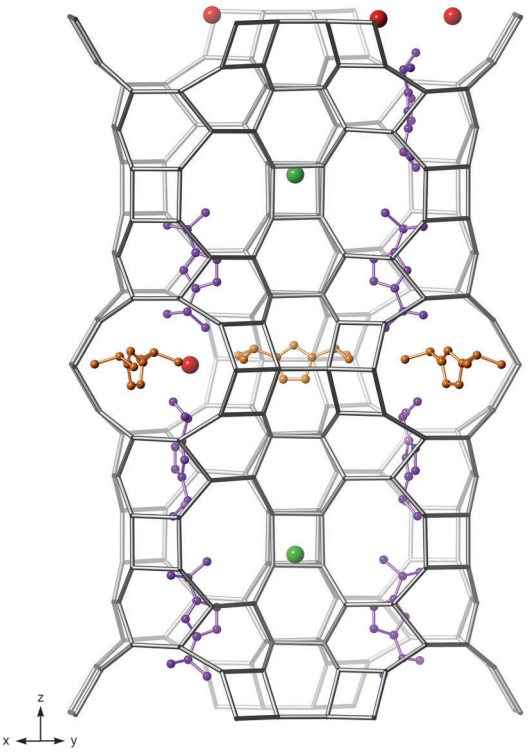

Fig. 5 Two neighboring channels A showing a possible arrangement of DIPI-3 (purple), DIPI-4 (orange), the fluoride ions (green balls) and the water molecules (red balls). Framework oxygen atoms have been omitted for clarity.

Fluoride ions were found off the center of the *d*4*r* units with a population of 0.33 (4 per unit cell). That is, two of the six *d*4*r*'s per unit cell are empty. At this stage there was still some residual electron density in the channels, and that was attributed to water, but could also be hydroxide or fluoride ions. Two positions were found in channel A, one close to DIPI-3 and a second close to DIPI-4, so the occupancy factors were adjusted to avoid any unreasonably close contacts. Two more positions were located in the smaller cavity of channel B, to give a total of 29.8 H_2O molecules (or OH^- or F^- ions) per unit cell.

Refinement of this model with geometric restraints on the bond lengths and angles of the framework yielded a reasonable geometry and a good profile fit. The crystallographic data for this model are given in Table 3, the profile fit in Fig. 6, and a cif in the ESI.†

Discussion

The structure of Zn-DAF-1 synthesized with DIPI adopts the same symmetry as that reported for the metalloaluminophosphates

Table 3 Crystallographic data from the Rietveld refinement of Zn-DAF-1[a]

Refined chemical composition	$\lvert(DIPI)_{17.2}F_{4.0}(H_2O,OH,F)_{29.8}\rvert [Zn_{6.1}Al_{125.9}P_{132}O_{528}]$
Unit cell	
a	22.2244(1) Å
c	42.3293(3) Å
Space group	$P6/mcc$
Standard peak (hkl, °2θ)	110, 5.16
Peak range (FWHM)	18
Data points	9970
Contributing reflections	1290
Geometric restraints	220
P–O 1.52(1) Å	46
Al–O 1.74(1) Å	46
O–T–O 109.5(8)°	68
T–O–T 145(8)°	23
C–N[b] 1.35/1.50(1) Å	21
C–C[c] 1.36/1.53(1) Å	20
C–N–C[d] 108/126(2)°	18
C–C–C 109.5(20)°	6
C–C–N[e] 108.0/109.5(20)°	18
Parameters	
Positional	
Framework + F	103
DIPI + O_w	83
Profile	11
R_F	0.144
R_{wp}	0.113
R_{exp}	0.050

[a] The numbers given in parentheses are the estimated standard deviations (esd's) in the units of the least significant digit given. Each restraint was given a weight equivalent to the reciprocal of its esd. [b] 1.35 Å in the imidazolium ring and 1.50 Å for the isopropyl group. [c] 1.36 Å in the imidazolium ring and 1.53 Å for the isopropyl group. [d] 108° in the imidazolium ring and 126° between the ring and the isopropyl group. [e] 108° in the imidazolium ring and 109.5° between the ring and the isopropyl group.

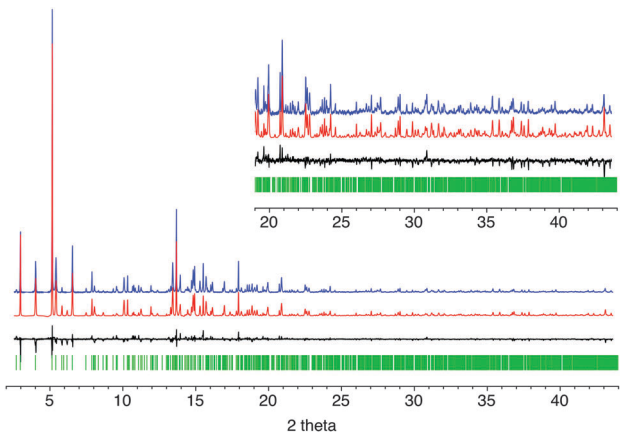

Fig. 6 Observed (black), calculated (red) and difference (blue) profiles for the Rietveld refinement of Zn-DAF-1. The profiles in the inset have been scaled up by a factor of 5 to show more detail. Reflection positions are marked as vertical bars.

Mg-DAF-1 and CoMg-DAF-1 synthesized with DM as the SDA.[14] The structure of Mg-DAF-1 was solved originally from laboratory single-crystal diffraction data in the space group $P6/mmm$ (c = 21.639 Å), where the Al and P sites are not distinguished. In a subsequent structure analysis using synchrotron single-crystal diffraction data,[23] super-lattice reflections that required a doubling of the c axis, were observed. This is consistent with a strict alternation of the Al and P atoms in the framework. The XPD data of Zn-DAF-1 described here also shows a few small peaks that require the doubled c axis (*e.g.* at 13.7 and 19.8° 2θ).

Even with the correct symmetry, finding the DIPI cations in the pores of Zn-DAF-1 was not straightforward, because the initial electron density maps showed only a few small clouds, and these did not have the shape of a DIPI cation (Fig. 3). The main difficulty was that the DIPI does not follow the high symmetry of the framework and it is therefore disordered. For example, DIPI-2, which lies in channel B aligned along the 6-fold axis, is disordered over 12 equivalent positions (generated by the 6-fold axis and the mirror plane perpendicular to it). Only one of these 12 can be occupied at any one time, so the electron density from one molecule is spread over 12 positions, not only making it difficult to interpret the shape of the cloud, but also diluting its intensity by a factor of 12. The disorder of DIPI-1, which is also located in the large cavity of channel B, is similar, but there, three of the 12 positions can be occupied simultaneously. Despite these difficulties, the coordinates of the DIPI cations could eventually be determined and refined approximately to yield 17.2 cations per unit cell, in good agreement with the chemical analysis (*ca.* 17 per unit cell). The refinement shows that DIPI-1 and DIPI-2 come close to filling all the space available in the large cavity of channel B, while the amount of DIPI-3 and DIPI-4 in channel A is somewhat lower and the void space is filled with water molecules, hydroxide and/or fluoride ions (1.5 close to DIPI-3 and 2.5 close to DIPI-4). The smaller cavity of channel B is similarly filled.

No evidence of octahedrally coordinated Al was found in the structure, so we assume that the signal at −6.3 ppm in the ^{27}Al MAS NMR spectrum and that at −140 ppm in the ^{19}F MAS NMR arise from an amorphous aluminofluoride impurity composed of octahedral Al sites with terminal Al–F units (see Fig. S3, ESI†).[19]

In Mg-DAF-1, channel A was found to be the preferred location for the DM species. A computational study[25] showed that the minimum energy configuration is that with the DM lying parallel to the c axis, in an orientation similar to that of DIPI-3. In view of the lower stability of the DM in channel B, it was concluded that the templating action is restricted to channel A and the DM cations in channel B are just filling the voids. The difference maps calculated using either set of single-crystal diffraction data could not be interpreted, and this was attributed to the disorder of the DM species. In channel B no peaks could be allocated, and even in channel A, only the amine groups could be assigned.

In Zn-DAF-1, we have found that two different DIPI positions, DIPI-1 and DIPI-2, are necessary to stabilize the large cavity, and they arrange themselves in a way that fills most of the available space. Three molecules of DIPI-1 form a circle around the inner walls of the cage, and DIPI-2 occupies the central part. With DIPI-3 located in channel A and DIPI-4 in the 10-ring windows connecting these channels, all four DIPI cations appear to play a structure-directing rather than just a space-filling role. This can be seen from the orderly packing of the Hirshfeld surfaces shown

in the ESI† (Fig. S4), and is perhaps why all DIPI positions could be determined, albeit with some degree of uncertainty. It is unusual for a single SDA to adopt more than one crystallographic position in a zeolite crystal structure, and to the best of our knowledge, this is the first time it has been observed in a structure analysis. In particular, it is very unusual for four cations to assemble into a "super SDA", such as that found in the large cavity, but the good fit inside the cage shown in Fig. 4 indicates that this cluster must be acting as an SDA and not just filling the space at random.

There are 6 Zn atoms per unit cell, and these are located at a single T-site in the 10-ring openings that connect neighboring channels A (Fig. 7). Of the four DIPI positions, only DIPI-4 makes relatively close contacts to framework O atoms (N42–O15 = 3.41 Å and N41–O12 = 3.44 Å), and O15 is connected to T5, where the Zn atoms are located, suggesting that the Zn location has also been guided by the SDA. This arrangement of the Zn atoms and the resulting P/Al ratio (132/126 = 1.05) is fully consistent with the ^{31}P NMR results.

The amount of Zn in Zn-DAF-1 (Zn/P = 0.046) is much lower than that of Mg in Mg-DAF-1 (Mg/P = 0.22). The two structures contain similar numbers of SDA species (15.8 DM per unit cell in Mg-DAF-1 and 17.2 DIPI in Zn-DAF-1), but the DM cations have two positive charges, whereas the DIPI cations have only one. This, and the presence of fluoride ions, which were not used in the synthesis of Mg-DAF-1, probably account for the fact that the amount of heteroatom replacing Al is much lower in Zn-DAF-1 than in Mg-DAF-1. The four fluoride ions found in the *d*4*r*'s plus the 6 Zn atoms add up to 10 negative charges per unit cell, a number considerably smaller than the 17.2 positive charges from the DIPI. The excess positive charge is probably balanced by fluoride or hydroxide ions located at some of the positions refined as water molecules.

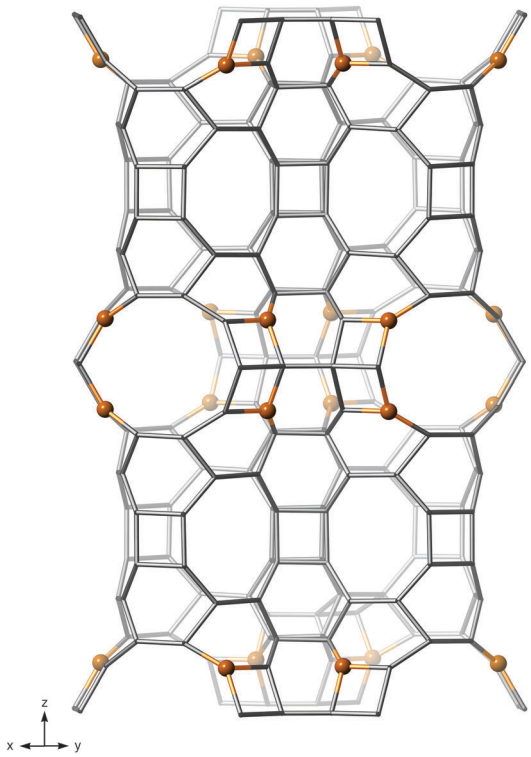

Fig. 7 Two neighboring channels A highlighting the Al5 site (orange balls) in the 10-ring openings that connect each channel A with three neighboring channels A. In each unit cell, there are 6 Zn atoms and 18 Al atoms in this site.

Conclusions

An ionic liquid approach to molecular sieve synthesis using *N*,*N*′-di-isopropyl-imidazolium (DIPI) in a zincoaluminophosphate system in the presence of HF has produced a novel material with an open **DFO**-type framework structure. Both chemical analysis and the ^{13}C NMR spectrum indicate that the DIPI structure directing agent remains intact in the final product. By performing a careful structure analysis, we were able to locate the extra framework species and the Zn atoms in this Zn-DAF-1 material. The DIPI cations were found to adopt four crystallographically distinct positions that filled the channels in an ordered and efficient manner. In addition to these positions, one fluoride and four $H_2O/OH^-/F^-$ positions were also found. The arrangement of these extra-framework species within the framework structure minimizes the amount of empty space within the channels, and the fact that the DIPI species appear to be well ordered suggests that they play a structure-directing role in the formation of Zn-DAF-1. This is in contrast to the case of Mg-DAF-1, where it was concluded that the decamethonium cations were disordered and that only those in channel A were likely to have any templating effect. All Zn atoms in Zn-DAF-1 were found in a single T site in the 10-ring apertures connecting neighboring channels A. The amount of Zn (6 per unit cell) is much lower than that of Mg in Mg-DAF-1 (29 per unit cell), and this may explain why the material appears to be more thermally stable. Thus, by combining information from synchrotron powder diffraction data, solid state NMR and chemical analysis, it has been possible to learn some of the finer details of the structure of Zn-DAF-1 and thereby better understand its synthesis and properties.

Acknowledgements

The authors thank Nicola Casati and Antonio Cervellino from the Material Science beamline at SLS in Villigen, Switzerland, for their assistance with the powder diffraction measurement. A. B. P. thanks Chevron ETC for financial support. The NMR facility at Caltech was supported by the National Science Foundation (NSF) under Grant Number 9724240 and partially supported by the MRSEC Program of the NSF under Award Number DMR-520565.

Notes and references

1 E. R. Cooper, C. D. Andrews, P. S. Wheatley, P. B. Webb, P. Wormald and R. E. Morris, *Nature*, 2004, **430**, 1012.
2 E. R. Parnham and R. E. Morris, *Acc. Chem. Res.*, 2007, **40**, 1005.
3 S. I. Zones, *Zeolites*, 1988, **8**, 483.

4 R. Archer, S. I. Zones and M. E. Davis, *Microporous Mesoporous Mater.*, 2010, **130**, 255.
5 S. I. Zones and A. W. Burton, *US Pat.*, 7,108,843, 2006.
6 I. Ogino, E. A. Eilertsen, S.-J. Hwang, T. Rea, D. Xie, X. Ouyang, S. I. Zones and A. S. Katz, *Chem. Mater.*, 2013, **25**, 1502.
7 R. Runnebaum, X. Ouyang, J. A. Edsinga, T. Rea, L. Arslan, S.-J. Hwang, S. I. Zones and A. S. Katz, *ACS Catal.*, 2014, **4**, 2364.
8 J. Schmidt, S. I. Zones and M. E. Davis, *Microporous Mesoporous Mater.*, 2014, **200**, 132.
9 J. Schmidt, M. W. Deem and M. E. Davis, *Angew. Chem.*, 2014, **126**, 8512.
10 A. B. Pinar, L. B. McCusker, C. Baerlocher, J. E. Schmidt, S.-J. Hwang, M. E. Davis and S. I. Zones, *Dalton Trans.*, 2015, **44**, 6288.
11 J. E. Schmidt, D. Xie, T. Rea and M. E. Davis, *Chem. Sci.*, 2015, **6**, 1728.
12 P. S. Wheatley, P. K. Allan, S. J. Teat, S. E. Ashbrook and R. E. Morris, *Chem. Sci.*, 2010, **1**, 483.
13 C. Baerlocher, L. B. McCusker and D. H. Olson, *Atlas of Zeolite Framework Types*, Elsevier, Amsterdam, 2007; C. Baerlocher and L. B. McCusker, Database of Zeolite Structures, http:// www.iza-structure.org/databases/.
14 P. A. Wright, R. H. Jones, S. Natarajan, R. G. Bell, J. Chen, M. B. Hursthouse and J. M. Thomas, *Chem. Commun.*, 1993, 633.
15 Composite building units found in more than one framework type have been assigned three letter codes (italic small letters), which are listed in ref. 13.
16 S. I. Zones, *US Pat.*, 4,483,835, 1984.
17 P. R. Willmott, D. Meister, S. J. Leake, M. Lange, A. Bergamaschi, M. Boege, M. Calvi, C. Cancellieri, N. Casati, A. Cervellino, Q. Chen, C. David, U. Flechsig, F. Gozzo, B. Henrich, S. Jaeggi-Spielmann, B. Jakob, I. Kalichava, P. Karvinen, J. Krempasky, A. Luedeke, R. Luescher, S. Maag, C. Quimann, M. L. Reinle-Schmitt, T. Schmidt, B. Schmitt, A. Streun, I. Vartiainen, M. Vitins, X. Wang and R. Wullschleger, *J. Synchrotron Radiat.*, 2013, **20**, 667.
18 C. Baerlocher and A. Hepp, *XRS-82, The X-ray Rietveld System*, Institut für Kristallographie, ETH Zürich, Switzerland, 1982.
19 C. Schott-Darie, J. Patarin, P. Y. Ge Goff, H. Kessler and E. Benazzi, *Microporous Mater.*, 1994, **3**, 123.
20 L. Sierra, C. Deroche, H. Gies and J. L. Guth, *Microporous Mater.*, 1994, **3**, 29.
21 P. E. Werner, L. Eriksson and M. Westdahl, *J. Appl. Crystallogr.*, 1985, **18**, 367.
22 B. H. Toby, *J. Appl. Crystallogr.*, 2005, **38**, 1040.
23 G. Muncaster, G. Sankar, C. R. A. Catlow, J. M. Thomas, R. G. Bell, P. A. Wright, S. Coles, S. J. Teat, W. Clegg and W. Reeve, *Chem. Mater.*, 1999, **11**, 158.
24 C. Baerlocher and A. Hepp, *Z. Kristallogr.*, 1976, **144**, 415.
25 P. A. Wright, C. Sayag, F. Rey, D. W. Lewis, J. D. Gale, S. Natarajan and J. M. Thomas, *J. Chem. Soc., Faraday Trans. 1*, 1995, **91**, 3537.

